PROCEEDINGS OF SCIENCE

The eigenvalue spectrum for dynamical Chirally Improved fermions

Martina Joergler* **and C. B. Lang**
Institut für Physik, FB Theoretische Physik, Universität Graz, A-8010 Graz, Austria
E-mail: martina.joergler@edu.uni-graz.at, christian.lang@uni-graz.at

We study the eigenvalues of Dirac operators in QCD with two mass degenerate dynamical fermions. The gauge configurations have been obtained with HMC and the so-called Chirally Improved fermionic action. We compare eigenvalues obtained for the overlap Dirac operator on these configurations with those for the Chirally Improved (CI) operator (studied earlier). Results of Random Matrix Theory allow us to determine the chiral condensate.

The XXV International Symposium on Lattice Field Theory
July 30 - August 4 2007
Regensburg, Germany

*Speaker.

PoS(LATTICE 2007)107

1. Dirac operators: D_{WI}, D_{OV}, and D_{CI}

In this work we compare the properties of the eigenvalue spectra of three lattice Dirac operators, namely the Wilson operator D_{WI}, the overlap operator D_{OV} and the Chirally Improved (CI) operator, denoted as D_{CI}. The well known D_{WI} (for vanishing mass parameter m) is given by

$$D_{\mathrm{WI}}(m,n) = \frac{4}{a}\mathbf{1} - \frac{1}{2a}\sum_{\mu=\pm1}^{\pm4}(\mathbf{1}-\gamma_\mu)\,U_\mu(n)\,\delta_{n+\hat{\mu},m}\,, \tag{1.1}$$

using the notation $\gamma_{-\mu} = -\gamma_\mu$. The operator violates chiral symmetry, and thus does not satisfy the Ginsparg-Wilson equation. The second fermionic action studied here is defined through D_{OV} [1]:

$$D_{\mathrm{OV}} = \frac{1}{a}\left(\mathbf{1} - \gamma_5\,\mathrm{sign}(\gamma_5\,\mathrm{A})\right)\,, \tag{1.2}$$

with $A = \mathbf{1}\,s - a\,D_{\mathrm{WI}}$ and $0 < s < 2$. For our calculations, we chose $s = 1.8$.

This operator is an exact solution of the Ginsparg-Wilson equation

$$\gamma_5 D + D\gamma_5 = D\gamma_5 D\,, \tag{1.3}$$

and therefore implements chiral symmetry on the lattice. As a consequence of this the spectrum of D_{OV} lies exactly on a circle, the so-called Ginsparg-Wilson circle.

The third Dirac operator we used, D_{CI}, represents an approximate solution to (1.3). It is defined [2] as a truncated expansion of a most general solution of the Ginsparg-Wilson equation into 'paths' on the lattice of varying length. Taking paths up to infinite length results in an exact solution. Using this technique we can combine lower computer cost with – approximate, but good – chiral properties [3].

2. Dynamical Chirally Improved fermions

For the following analysis of the spectral properties of the Dirac operators we use gauge fields with 2 dynamical flavors of fermions with degenerate masses. These were constructed with an HMC-algorithm, implemented with the Lüscher-Weisz gauge action and the already mentioned CI fermionic action. More details can be found in [5].

Due to the 'almost chiral' properties of this action, our HMC produces gauge-configurations which frequently tunnel between different topological sectors within one Markov chain. Table 1 gives a short summary of the parameters of the gauge fields used in our analysis.

3. Comparison of the spectral properties

Inspection of the spectrum of a Dirac operator is a very good method to see how well chiral symmetry is approximated. In Fig. 1, for example, it can be clearly seen that the CI spectrum (right) deviates less from the ideal Ginsparg-Wilson circle than that of D_{WI} (left).

Another information the spectrum provides is the topological charge Q_{top} of a gauge configuration. According to the Atiyah-Singer index theorem it is possible to determine Q_{top} by counting the zero modes of a Ginsparg-Wilson type Dirac operator according to their chirality,

$$Q_{top} = n_- - n_+ \tag{3.1}$$

run	$L^3 \times T$	β_1	am	a[fm]	am_{AWI}	#confs.
a	$12^3 \times 24$	5.2	0.02	0.115(6)	0.025	73
b	$12^3 \times 24$	5.2	0.03	0.125(6)	0.037	52
c	$12^3 \times 24$	5.3	0.04	0.120(4)	0.037	55
d	$12^3 \times 24$	5.3	0.05	0.129(1)	0.050	40

Table 1: The parameters for the runs used for this work. $L^3 \times T$ denotes the extent of the lattice in units of the lattice spacing a, am the bare mass parameter of D_{CI}, am_{AWI} the quark mass calculated via the axial Ward identities, and β_1 the first gauge coupling of the set of three LW-couplings used [5]. The configurations are separated by 10 HMS-trajectories.

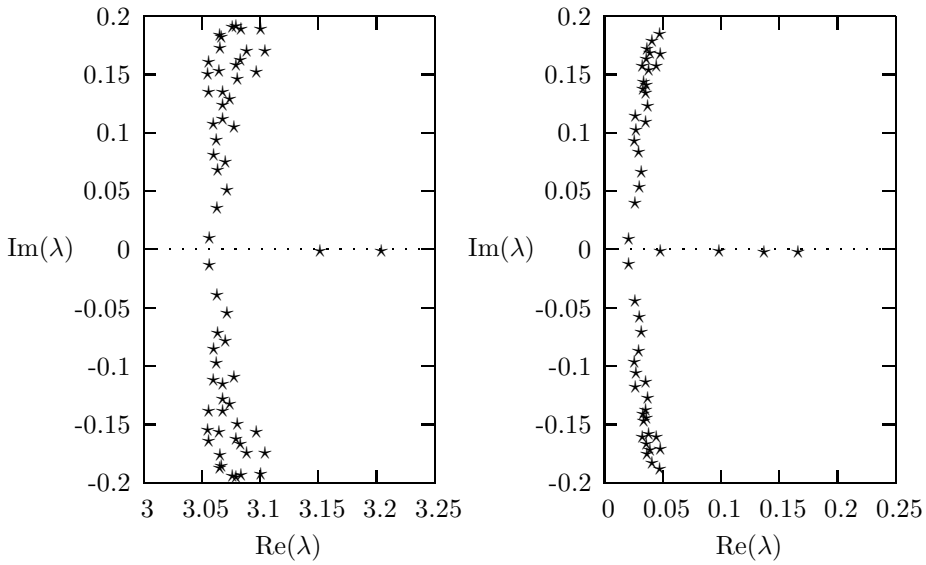

Figure 1: Left: Part of the spectrum of D_{WI} for configuration nr. 100 of run a. Right: The 50 smallest eigenvalues of D_{CI} for the same gauge-configuration.

with $n_\pm$ denoting the number of eigenmodes $|v\rangle$ with chirality $\langle v|\gamma_5|v\rangle = \pm 1$ corresponding to eigenvalues $\lambda = 0$. When treating D_{CI}, due to its approximate nature, these eigenvalues are not exactly zero, but scatter on the real axis. For the CI operator (and the Wilson operator) one may relate the number of real modes to the topological sector. We determine Q_{top} by setting $n_\pm$ as the number of eigenmodes $|w\rangle$ corresponding to real eigenvalues with chirality $\langle w|\gamma_5|w\rangle \gtrless 0$, respectively. (For eigenvalues not on the real axis we numerically find $\langle w|\gamma_5|w\rangle = 0$ as expected.) When comparing the topological charge of a configuration calculated with the exactly chiral D_{OV} and the approximately chiral D_{CI}, and we find approximate agreement (cf. Fig. 2). The differences mostly originate from missed eigenvalues far inside the Ginsparg-Wilson circle, which are not recovered in our method of calculating eigenvalues, namely the program package ARPACK; this tool only computes the eigenvalues with the smallest absolute value with respect to a defined origin. When computing eigenmodes of the overlap operator, the situation is different. There the sector depends on the value of s added to the diagonal part of the kernel operator (Wilson in our case), which has frequent inner real modes that are missed in that overlap projection, depending on s.

If one does not take into account any normalization and directly compares eigenvalues of D_{CI} with those of D_{OV} as defined in (1.2), an interesting behavior can be seen. In cases where not only

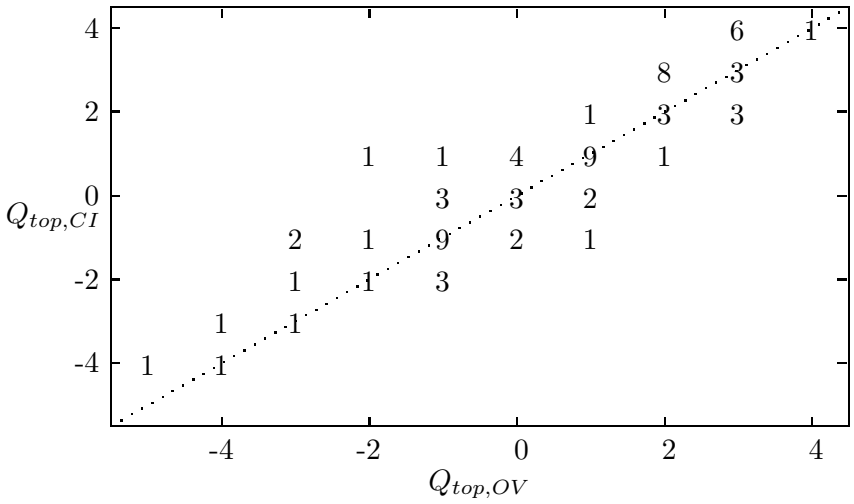

Figure 2: $Q_{top,OV}$ vs. $Q_{top,CI}$ for the gauge configurations of run a. The numbers state how many configurations show a particular combination of topological charges.

the topological charge Q_{top} is identical for both operators but also the number of real eigenvalues n_0, the first few eigenvalues are in direct correspondence (cf. Fig. 3, left). However, if $n_0 > Q_{top}$ for the CI operator, i.e., if eigenmodes with opposite chirality cancel each other with respect to Q_{top}, this correspondence is lost (cf. Fig. 3, right). When put into the overlap operator, the real modes seem to "move" up resp. down the imaginary axis (although not all of them close to the real axis), thereby increasing the eigenvalue density near the origin. For a similar observation cf. [4]. This enhancement leads to a higher value for the (bare) chiral condensate when calculated directly with this definition of D_{OV}.

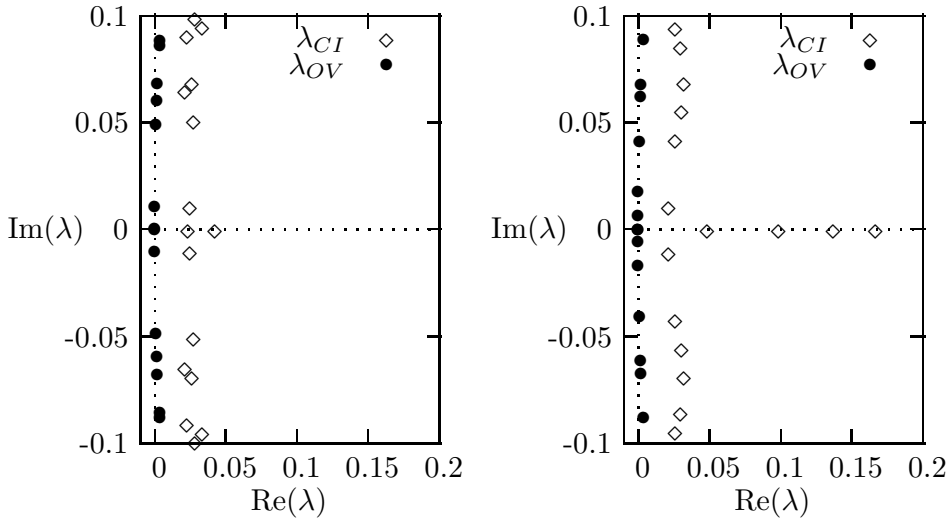

Figure 3: Eigenvalues λ_{OV} of D_{OV} and eigenvalues λ_{CI} of D_{CI} in the complex plane. Left: configuration nr. 110 (run (a)): $Q_{top} = -2$, $n_+ = 2$ for both operators Right: configuration nr. 100 (run (a)): $Q_{top} = -2$, but $n_{+,CI} = 3$, $n_{-,CI} = 1$.

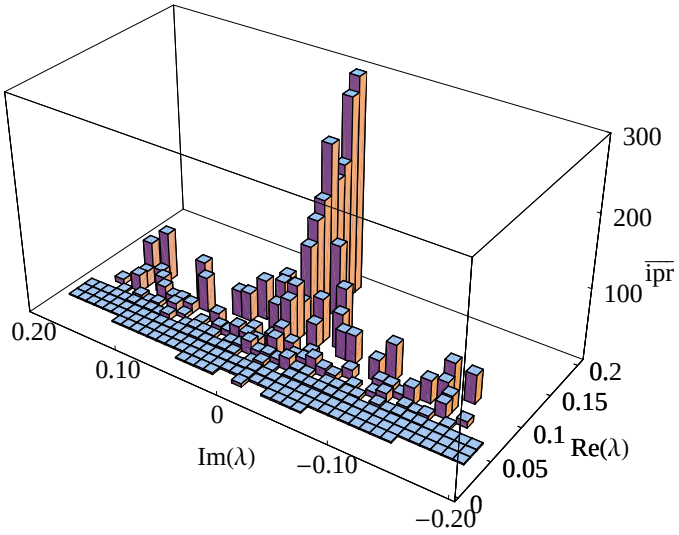

Figure 4: The average value $\overline{ipr}(\lambda)$ over the complex plane for the gauge configurations of run (a).

4. Localization of eigenmodes

For the CI operator, we also calculated the inverse participation ratios (ipr) of the eigenmodes for small eigenvalues, given by

$$ipr(\lambda) = V \sum_x \left(\sum_{\alpha,c} v(x,\alpha,c)^* v(x,\alpha,c) \right)^2 . \tag{4.1}$$

The inner sum is over the color indices c as well as the Dirac indices α, the outer sum over the space-time indices x. V denotes the space-time volume in lattice units, and $v(x,\alpha,c)$ the eigenmode of D_{CI} corresponding to the eigenvalue λ. This quantity is a good measure for the localization properties of one eigenmode, with $ipr(\lambda) = 1$ for a non-localized mode and $ipr(\lambda) = V$ for a mode concentrated on only one lattice point. To compute a suitable average over one HMC-run, we divided the complex plane into a grid and calculated the average ipr as

$$\overline{ipr} = \frac{1}{n} \sum_{\lambda \in \Delta_\lambda} ipr(\lambda) , \tag{4.2}$$

with Δ_λ being one square in the complex plane and n the number of eigenvalues in Δ_λ.

In Fig. 4 we see, as expected, that $\overline{ipr}$ increases along the real axis, and in general is higher for eigenvalues inside the Ginsparg-Wilson circle (cf. also [4]). For D_{OV} one expects $\overline{ipr}$ to be symmetric with respect to the real axis, but this is not the case for D_{CI} since it is not a normal matrix operator.

5. Comparison with random matrix theory

As the overlap operator implements chiral symmetry on the lattice exactly, the distribution of the smallest eigenvalues (in leading order ChPT) is analytically given by the well known results of

random matrix theory (RMT) for the chiral gaussian unitary ensemble [6], at least in the ε-regime in the microscopic limit. Following the procedure in [7], where these calculations were done on the same configurations for D_{CI}, we thus compare our distributions for D_{OV} to RMT.

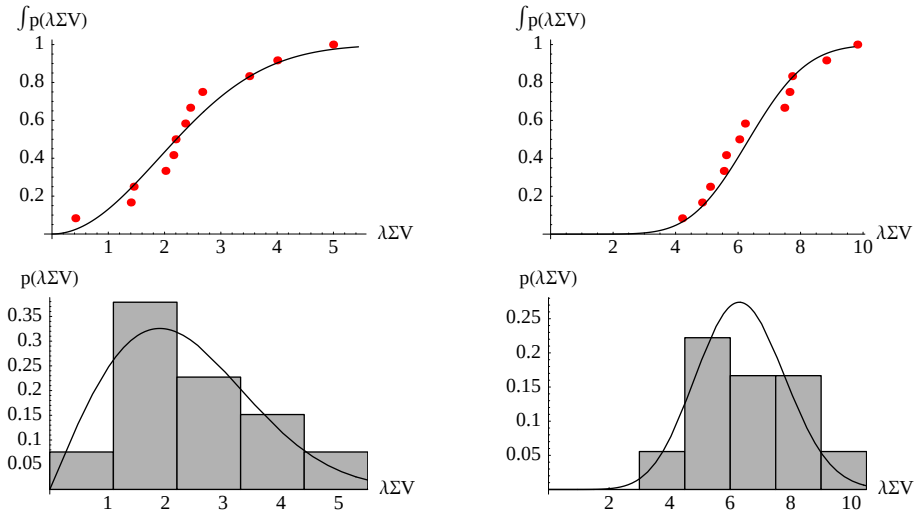

Figure 5: The cumulative distribution given by RMT compared to the distribution of the smallest eigenvalues of the overlap operator. Left: $Q_{top} = 0$, and k=1 (smallest eigenvalue); Right: $Q_{top} = 0$, and k=2 (second smallest eigenvalue), both for run (a).

A similar analysis for dynamical overlap configurations was done in [8, 9] and for 2-flavor staggered configurations in [10]. For the fits that determine the chiral condensate Σ, we use the cumulative eigenvalue distributions and look at the smallest and second smallest eigenvalue in the topological sectors $Q_{top} = 0$ and $|Q_{top}| = 1$.

The values for Σ for run (a)–(d), determined from the spectra of D_{OV}, are given in Table 2. The fit was done using the Kolmogorov-Smirnov test, the errors computed via statistical bootstrap.

6. Problems and issues

The resulting values for the condensate still have to be renormalized. This can be done by determining the renormalization constant Z_S by standard tools of non-perturbative renormalization. In the case of D_{CI} the renormalization constants for the dynamical case have been computed in recent work [11]. For D_{OV}, the situation is more involved, and the renormalization depends on the value of s. The weak coupling expansion for small momenta p has a behavior $D_{\mathrm{OV}} = i\,\gamma_\mu p_\mu / s + \mathcal{O}(p^2)$. This changes for the interacting case in a non-trivial way. Comparing the results for the bare condensate for CI [5] with overlap, we expect $Z_{S,OV} = Z_{S,CI}\,\Sigma_{CI}/\Sigma_{OV} \approx 0.64 Z_{S,CI}$.

The dependence on the physical quark mass is also worth being explored. To this point we assume that the AWI-mass computed for our dynamical gauge fields is the same as the quark mass entering the RMT-fits. In [10] the overlap quark mass has been determined using the distribution of topological charge, and found to be different from the value calculated for the underlying gauge fields. We do not have sufficiently high statistics to follow this approach, but nevertheless the sea quark mass of the overlap operator should be adjusted, such that the pion mass (or the AWI-mass) computed with the overlap operator agree with the pion mass of the CI operator.

HMC run	k	$\lvert Q_{top}\rvert$	#confs.	$-\langle\Sigma\rangle^{1/3}$ MeV$^{1/3}$
a	1	0	12	338(6)
	1	1	25	332(3)
	2	0	12	310(3)
	2	1	25	319(3)
b	1	0	7	353(10)
	1	1	8	350(9)
	2	0	7	362(5)
	2	1	8	330(6)
c	1	0	17	350(6)
	1	1	12	346(9)
	2	0	17	340(3)
	2	1	12	322(5)
d	1	0	5	365(18)
	1	1	11	370(10)
	2	0	5	348(14)
	2	1	11	346(2)

Table 2: Results for the value of the bare condensate Σ, for all runs of the HMC. The value of k refers to the smallest (1) or second smallest (2) (imaginary part of the) eigenvalue.

Acknowledgments

Fruitful discussions with C. Gattringer, A. Hasenfratz and P. Majumdar are gratefully acknowledged. M.J. wants to thank the Paul Urban-Stiftung for financial support.

References

[1] H. Neuberger, *Phys. Lett.* **B417** (1998) 141 [hep-lat/9707022]; *ibid.*. **B427** (1998) 353 [hep-lat/9801031].

[2] C. Gattringer, *Phys. Rev.* **D63** (2001) 114501 [hep-lat/0003005]; C. Gattringer, I. Hip, and C.B. Lang, *Nucl. Phys.* **B597** (2001) 451 [hep-lat/0007042].

[3] C. Gattringer *et al.*, *Nucl. Phys.* **B677** (2004)3 [hep-lat/0307013].

[4] A. Hasenfratz, R. Hoffmann, and S. Schaefer (2007) [arXiv:0709.0932].

[5] C. B. Lang, P. Majumdar, and W. Ortner, *Phys. Rev.* **D73** 034507 (2006) 034507 [hep-lat/0512014].

[6] P. H. Damgaard and S. M. Nishigaki, *Phys. Rev.* **D63** 045012 (2001) 045012 [hep-th/0006111].

[7] C. B. Lang, P. Majumdar, and W. Ortner, *Phys. Lett.* **B649** (2007) 225 [hep-lat/0611010].

[8] T. DeGrand, Z. Liu, and S. Schaefer, *Phys. Rev.* **D74** (2006) 094504 [hep-lat/0608019]. [

[9] H. Fukaya *et al.*, (2007) [arXiv:0705.3322v1].

[10] A. Hasenfratz and R. Hoffmann, PoS(LAT2006)210 [hep-lat/0609070]; *Phys. Rev.* **D74** (2006) 114509 [hep-lat/0609067].

[11] Ph. Huber, to be published.